STATUS OF THE PLANAR UNDULATOR APPLIED IN HUST THz-FEL OSCILLATOR

B. Qin*, L. Yang, X.L. Liu, K.F. Liu, J. Yang, P. Tan, Y.Q. Xiong, X. Lei, Y.B. Wang
State Key Laboratory of Advanced Electromagnetic Engineering and Technology
Huazhong University of Science and Technology, Wuhan 430074, Hubei, China

Abstract

To fulfill the physical requirement of a 50-100 μm Free Electron Laser (FEL) oscillator, design considerations of a planar undulator are described. Some technical issues, including the tolerances study, the beam match, the field measurement setup and the influence on the magnetic field by the waveguide are discussed as well.

INTRODUCTION

In the past decade, terahertz (THz) science and technology has been developed rapidly. In applications of real-time imaging, security inspection, materials and biomedicals, high power compact THz sources with Watt level average power are demanded[1], which is beyond capability of traditional THz sources.

A prototype compact terahertz FEL oscillator was proposed at Huazhong University of Science and Technology (HUST), which is designed to generate $50-100\mu m$ coherent radiation with 1 MW level peak power[2]. The conceptual design is shown in Fig. 1, with the main design parameters listed in Table 1. We choose a thermionic electron gun with an independently tunable cell (ITC) as the electron beam source for simplicity, with output energy around 2MeV[3]. A S-band linac with traveling wave structure will accelerate the beam to range of 6 MeV to 14 MeV, that covers the energy from 8.1 to 11.7 MeV. The macro pulse duration $5\mu s$ is long enough for the power build up process which is around $1\mu s$. A symmetrical near-concentric optical cavity is formed by two gold-coated copper toroid mirrors, with the cavity length of 2.93m. A planar undulator with a moderate K is adopted. This paper mainly describes the physical parameters determination and technical aspect of the undulator.

Table 1: Parameters of the THz FEL Oscillator.

Beam energy	8.1-11.7 MeV
Radiation wavelength,λ_r	50 - 100 μm
Bunch charge	$\geq$ 200pC
Bunch length (FWHM),σ_s	5-10ps
Energy spread (FWHM)	0.3%
Normalized Emmittance,ϵ_n	$15\pi mm\cdot mrad$
RF	2856 MHz
Macro pulse duration	4-6 μs
Repetition rate	10-200Hz
Number of the full strength period,N_u	30
Undulator period,λ_u	32 mm
Undulator parameter,K	1.0-1.25
Optical cavity length	2.93m
Peak power	0.5-1 MW

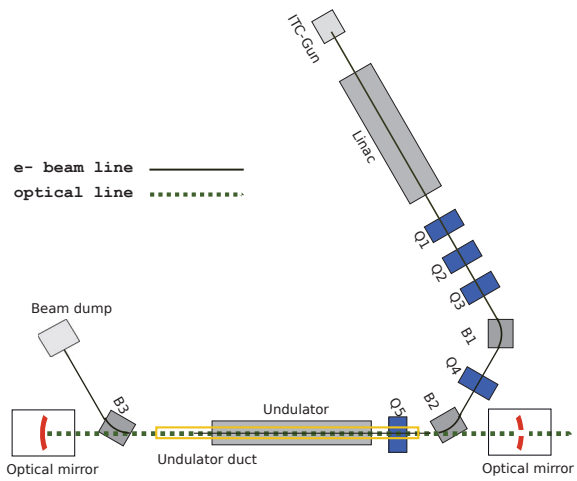

Figure 1: Schematic view of HUST THz-FEL oscillator.

DETERMINATION OF PARAMETERS

The evaluation of the FEL performance, including the gain, the saturated power and the saturation time is performed using 1D linear theory, and finally determined the undulator parameters based on the specification of the electron beam [2]. In the low gain FEL oscillator, the power build up process is non-linear and difficult to be described analytically. But the saturation time can be estimated with an analytical method[1]. The round-trip number m can be derived from the approximated exponential growth of the power build up $P_{sat} = P_0 \cdot (1 + G_{net})^m$, where $G_{net} = G_{max} - G_{loss}$ is the net round-trip gain with round-trip loss rate G_{loss} due to internal and transmission losses in the optical resonator.

$$m = \ln(P_{sat}/P_0)/\ln(1+G_{net}) = \ln n/\ln(1+G_{net}) \quad (1)$$

To achieve possible higher undulator peak field, the vertical aperture of the waveguide duct is 10mm, and the minimum gap size of the undulator $g = 16mm$. For a reasonable ratio $g/\lambda_u = 0.5$, the undulator period length $\lambda_u = 32mm$ is determined.

K is investigated from 1.0 to 1.5, and K_{max}=1.25 is determined. Compared to K=1.0, the gain is increased 35%, leading to 30% decrease of the saturation time and 20% increase of the saturation power. $K > 1.25$ brings insignifi-

* bin.qin@mail.hust.edu.cn

ISBN 978-3-95450-126-7

Copyright © 2013 CC-BY-3.0 and by the respective authors

cant enhancement of FEL performance, while asks for very high B_r for present undulator structure.

Choice of Optimum N_u

The period number N_u should be carefully chosen for long wave length FEL oscillator. Larger Nu brings higher gain, but introduces negative effect as well. For larger N_u, the radiation power is decreased due to the natural extraction efficiency $\frac{1}{4Nu}$, and smaller energy spread is required to keep same inhomogeneous factor - F_{inn}. N_u is scanned from 25 to 40, to observe the variation of the single pass gain and the saturation time, as shown in Fig. 2 and Fig. 3, and $N_u = 30$ is chosen. When N_u exceeds 30, there is no significant contribution to saturation time, but the optical power drops too much due to lower efficiency.

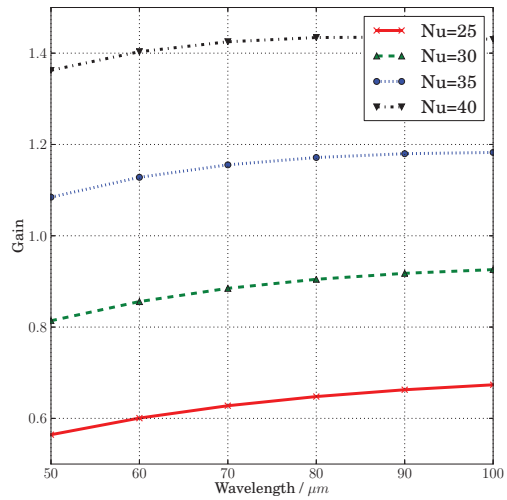

Figure 2: The maximum single pass gain versus radiation wavelength at different N_u

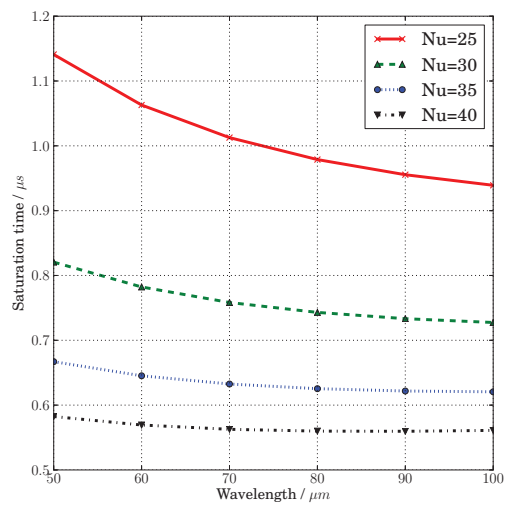

Figure 3: The saturation time versus radiation wavelength at different N_u, with 15% round trip loss assumed.

Undulator Structure

Compared to hybrid structure, pure permanent magnet (PPM) structure is chosen, due to: (1) Improved quality of PM materials, such as the deviation of polarization and spread of the remanent field B_r, and the field error due to materials inhomogeneity can be compensated by block sorting; (2) Better gap-dependence of performance related to undulator tolerances on integral fields and phase error etc.; (3) Easy for mechanical setup and assembling, leading to decrease of cost on the undulator construction.

For PPM undulators, to achieve $K_{max} = 1.25$ with $g/\lambda_u = 0.5$, a minimum remanent field $B_r = 1.2T$ is required, which is beyond the capability of SmCo. NdFeB is chosen for permanent magnet blocks. Historical literatures show that the SmCo has better irradiation resistance compared to NdFeB, due to higher coercivity. However, recent years, owing to development of PM technology, high coercivity grades ($H_{cj} > 20$kOe) of NdFeB can be provided.

Tolerances Study of the Undulator

Considering the FEL performance and achivable technical specifications, overall tolerances are listed in Table 2.

Table 2: Tolerances of the Undulator.

rms peak field error	$\leq 0.6\%$
rms period error	$\leq 0.2\%$
rms phase error	$\leq 3^\circ$
First integral(Normal/ Skew)	$\leq 1.2 \times 10^{-5}\mathrm{T}\cdot\mathrm{m}$
Second integral (Normal/ Skew)	$\leq 1.2 \times 10^{-5}\mathrm{T}\cdot\mathrm{m}^2$

For relative lower electron beam energy, small field integrals are required. With proposed tolerance of field integrals, electron offsets can be calculated as 0.5mm / 0.5mrad, that are confined within the beam cross section which is estimated to be σ_x=1mm, $\sigma_{x'} = 1.2$mrad.

For the rms peak field error, basic requirement is that the resulting inhomogeneous broadening in the gain spectrum due to the field error should be less than its natural width 1/2Nu, that asks for $\Delta B/B < 1.9\%$. Since other electron beam specifications will cause inhomogeneous broadening as well, a smaller tolerance 0.6% with one third of the estimation is chosen.

For tolerance of the phase error cause by the undulator field imperfection, one criterion is that it should be comparable to the phase error $\Delta\psi_{rms,spread} = 8^\circ$ due to the energy spread. As pointed out in [4], compared to the peak field error, the phase error is more meaningful since it has a strong correlation to the spontaneous emission and the small signal gain. Numerical simulations were performed to validate this correlation. By introducing different rms deviation of remanent field B_r in PM blocks, with 0.5% to 3% standard deviation, the field periodicity of the undulator is violated. Then the datasets containing the magnetic field are exported for analyzing the peak field error and phase shake. B2E[5] code was used for calculation of the spontaneous radiation. As shown in Fig. 4, the correlation is quite

ISBN 978-3-95450-126-7

Copyright © 2013 CC-BY-3.0 and by the respective authors

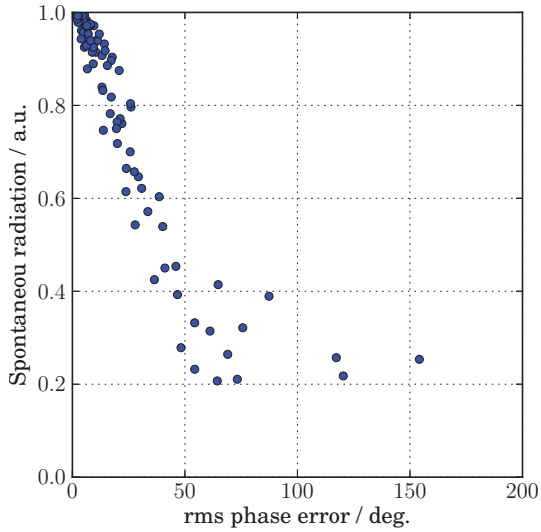

Figure 4: Relationship between the spontaneous radiation and phase error.

good in the range of 0 to 50 degrees. For the proposed tolerance 3°, the degradation of the spontaneous radiation is less than 2.5%.

UNDULATOR LATTICE AND BEAM MATCH

The radiation diffraction posses dominant factor in gain length growth especially for long wavelength FELs, due to comparable values between the beam cross section and the radiation wavelength. The dependence of the gain length on the average beta function is evaluated using M. Xie's formula[6], with the result shown in Fig. 5 [7]. This implies an achievable minimal average beta function is preferred to have a smaller gain length. The principle for beam matching is: 1) beam waist should be achieved at the center of the undulator, with a symmetrical distribution of the β function for both directions; 2) minimum values of β function and small fluctuation within the undulator for strongly focusing vertical direction.

For planar undulator, at the horizontal plane, since field gradient $k \approx 0$ in good field region, the very weak defocusing strength can be neglected and the undulator acts as a drift space. The beam waist (a minimum β_x with $\alpha_x = 0$) is desired at the undulator center. With a subscript notation '0' and '1' represents the start and end points of the undulator beam line, the matching condition asks for $\beta_{x,1} = \beta_{x,0}$ and $\alpha_{x,1} = -\alpha_{x,0}$. Using the transfer matrix of the drift space, we have

$$\beta_{x,0} = L \cdot (1 + \alpha_{x,0}^2)/2\alpha_{x,0} \tag{2}$$

where $L = 1.2\text{m}$ is the distance of the undulator beam line. From Equ. 2, a minimu $\beta_{x,0} = L$ can be derived when $\alpha_{x,0} = 1.0$, as a consequence $\beta_{x,mid} = L/2$ at the undulator center. And this condition is valid to all electron energy points.

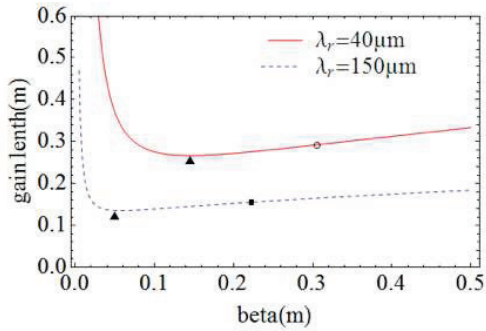

Figure 5: Gain length versus the average beta function for different radiation wavelength. The best value are marked with black triangle; The minimum average beta function value with natural focusing are marked with circle and black square.

The vertical plane presents focusing properties can be described with a vertical transfer matrix:

$$M_v = \begin{bmatrix} \cos(k_y z) & \frac{1}{k_y}\sin k_y z \\ -k_y \sin(k_y z) & \cos(k_y z) \end{bmatrix} \tag{3}$$

where $k_y = \frac{2\pi a_u}{\gamma \lambda_u}$. Then a constant and minimum beta function $\beta_y = 1/k_y$ can be found with the initial twiss parameters $\beta_{y,ent} = 1/k_y$, $\alpha_{y,ent} = 0$ at the entrance of the undulator. Since k_y is dependent on electron energy, the matching of the vertical twiss parameters should be related to the energy working point.

Using a numerical ray-tracing method, beam matching with both horizontal and vertical plane is performed. Two energy points: 8.1 MeV and 11.7 MeV are shown in Fig. 6. For the horizontal plane, the results match the theoretical prediction well, and neglectable difference between two energy points comes from the very weak defocusing effect. The vertical motion has a good match as well, with $\beta_{y,cen}$ very close to the theoretical value $\beta_y = 1/k_y$.

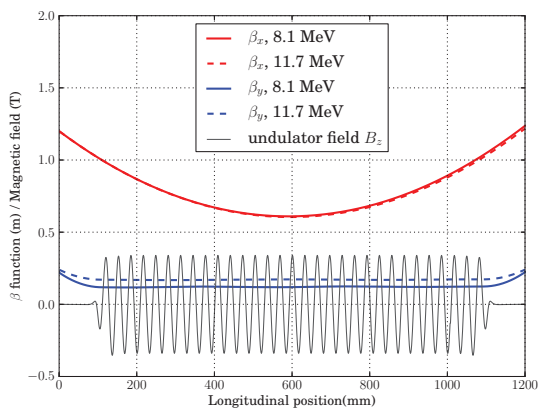

Figure 6: β function within the Nu=30, K=1.0 planar undulator, for 8.1 MeV and 11.7 MeV electron beam.

Copyright © 2013 CC-BY-3.0 and by the respective authors

ISBN 978-3-95450-126-7

INFLUENCE ON THE MAGNETIC FIELD OF THE WAVEGUIDE DUCT

A partial waveguide duct with inner cross section 10mm(V)×40mm(H) will be installed inside the planar undulator. A copper plated 316L stainless steel will be selected as the duct material. The nominal relative permeability of 316L $\mu_r = 1.02$, however during the machining and welding process, the permeability might change. To investigate this effect, a prototype duct was manufactured, and the measured $\mu_r \approx 1.1$. The influence on the magnetic field at the central line of the undulator was simulated by Cosmol (Fig. 7), with an increase of peak field about 8Gs [8].

The field difference for installing this prototype duct was measured by using a cartesian 2D mapping platform [9], with the result shown in Fig. 8. The platform was originally designed for mapping the mid-plane of the cyclotron and has a repetitive positioning error at the level of $10\mu m$, which caused a repetitive field mapping error (dataset A-B). The field increase at peak field is about 5Gs including this repetitive error, and a larger increase 10Gs is found to be located at left part of the duct close to the welding, which indicates a higher local permeability. The difference of the first field integrals is 7Gs·cm, which can be compensated by correction coils. However, for the formal waveguide duct, $\mu_r < 1.05$ should be guaranteed.

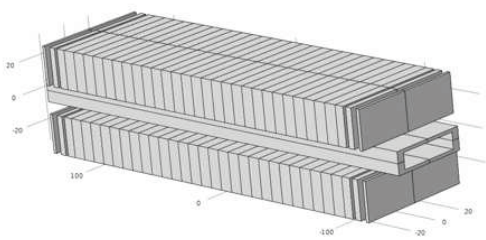

Figure 7: Model of the planar undulator with the waveguide duct.

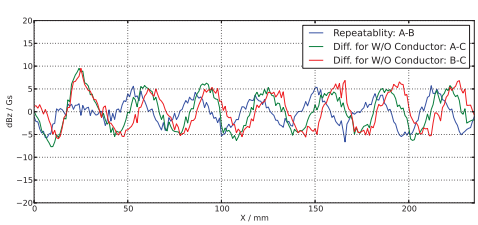

Figure 8: Measured field difference for with and without the waveguide duct. A,B: two datasets with the duct, for testing the measurement repeatability; C: dataset without the duct.

FAST FIELD INTEGRALS MAPPING SYSTEM

For fast online integral field measurement, some existing methods are considered. The pulsed wire method can measure the distribution of field integrals along the beam axis, however, the mapping result has a sensitive dependence on circumference factors and configuration of wire characteristics. We chose the stretch wire method for fundamental first and second field integrals mapping.

This system is under construction: Kohzu positioning stages XA10A-L2 / ZA16A-X1 are combined to fulfill 2D positioning, SC410 Controller provides maximum 4 axis synchronous motion control, with high repetitive positioning precision $2\mu m$; Agilent 3458A multimeter is used for voltage integration, with a 50 turn $80\mu m$ diameter Litz wire.

CONCLUSIONS

From views of physical and technical, design considerations of a planar undulator applied in a terahertz wave FEL oscillator are performed. Main undulator parameters and important tolerances of the undulator field quality are evaluated to ensure the performance of the radiation field under the designed electron beam specifications, with main goals of achieving 0.5-1 MW peak power at $50 - 100\mu m$ wavelength around $1\mu s$ saturation time.

We signed a contract with Kyma s.r.l, for undulator manufacture, and assembly is expected to be finished in the end of 2013.

REFERENCES

[1] Y. Socol, "High-power free-electron laserstechnology and future applications," Optics & Laser Technology, 46(2013), 111-126.

[2] B. Qin, P. Tan, L. Yang and X.L. Liu, "Design considerations of a planar undulator applied in a terahertz FEL oscillator," Nucl. Instrum. Meth. A 727 (2013) 90-96.

[3] Y.J. Pei et al., "R & D on a compact EC-ITC RF gun for FEL", Proceedings of IPAC 10, Kyoto, Japan, pp. 1737.

[4] B.L. Bobbs, G. Rakowsky, P. Kennedy et al., "In search of a meaningful field-error specification for wigglers," Nucl. Instr. Meth. A, 296(1990) 574-578.

[5] http://www.esrf.eu/Accelerators/Groups/InsertionDevices/Software/B2E

[6] M. Xie," Design optimization for an X-ray free electron laser driven by SLAC linac," Proceeding of PAC 1995, vol.1: 183-185.

[7] Lei Yang, Bin Qin, Jun Yang et al., "Optimization of the lattice function in the planar undulator applied for terahertz FEL oscillators," accepted by Chinese Physics C, 2013.

[8] Xialing Liu, Bin Qin, Lei Yang et al., "Influence of magnet errors and waveguide permeability on magnetic field performance in pure permanent undulators," Proceeding of IPAC 13, WEPWA038.

[9] J.Yang, et al., "Magnetic field measurement system for CYCHU-10," Proceeding of PAC09, pp.181-183.

ISBN 978-3-95450-126-7

Copyright © 2013 CC-BY-3.0 and by the respective authors